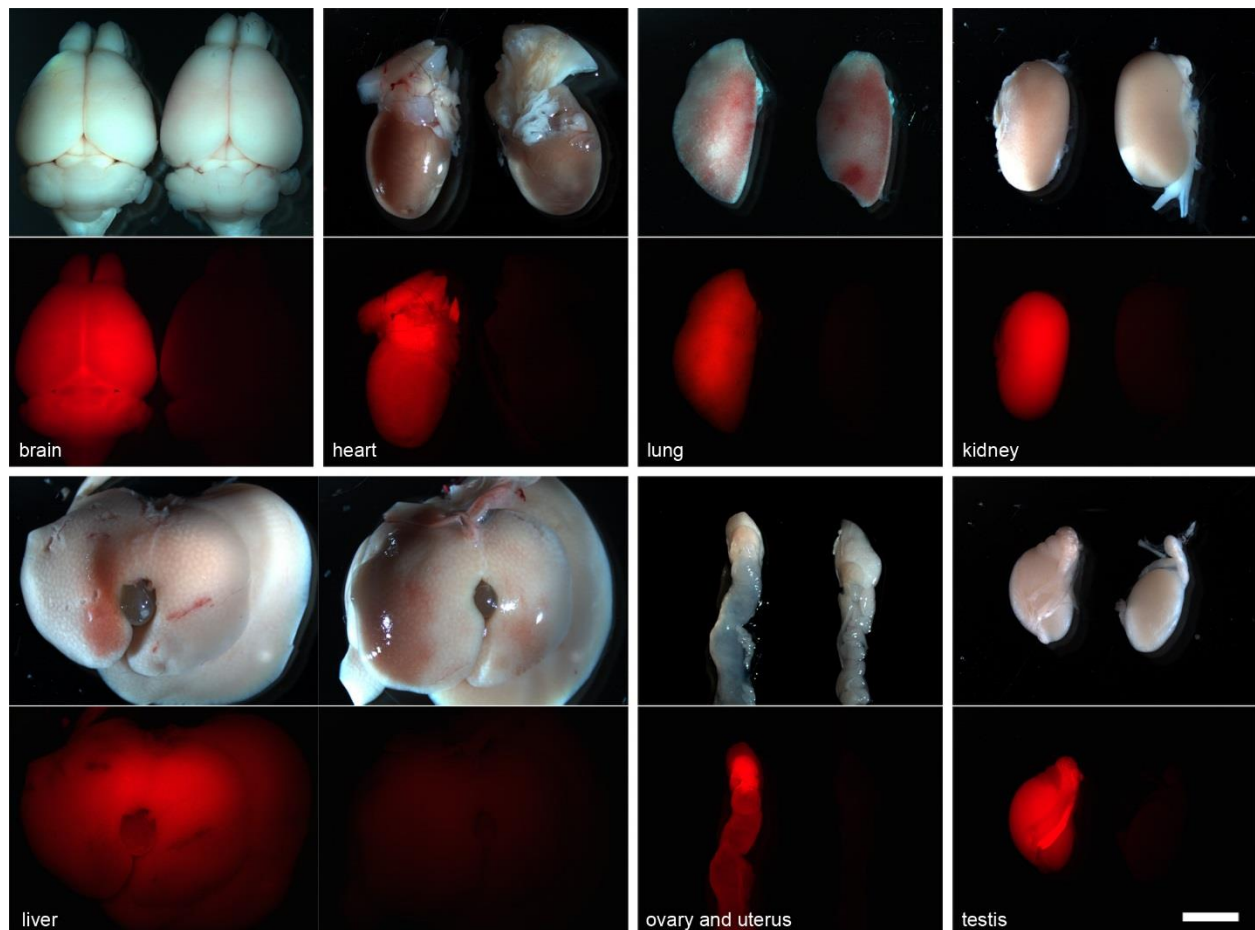## SUPPLEMENTARY FIGURES

Fig. S1. Cells in a wide variety of organs and tissues can be labeled by *RC::RFLTG* and its derivative alleles.

Ubiquitous activity of the CAG promoter in *RC::RFLTG* and its derivative alleles in a variety of organs is demonstrated by tdTomato fluorescence in 6-7 week old *CAG-Dre; ACTB-Flpe; RC::RFLTG* mice (left of each pair of organs, n=10). No fluorescence was seen in control organs (right of each pair, n=6) due to the presence of transcriptional stop cassettes (control brain, *RC::RFLTG*; other organs, *RC::RLTG*). **Top two rows, left to right:** Brain, heart, lung, kidney. **Bottom two rows, left to right:** liver, ovary and uterus, testis. Images show native fluorescence. Scale bar: 5 mm.
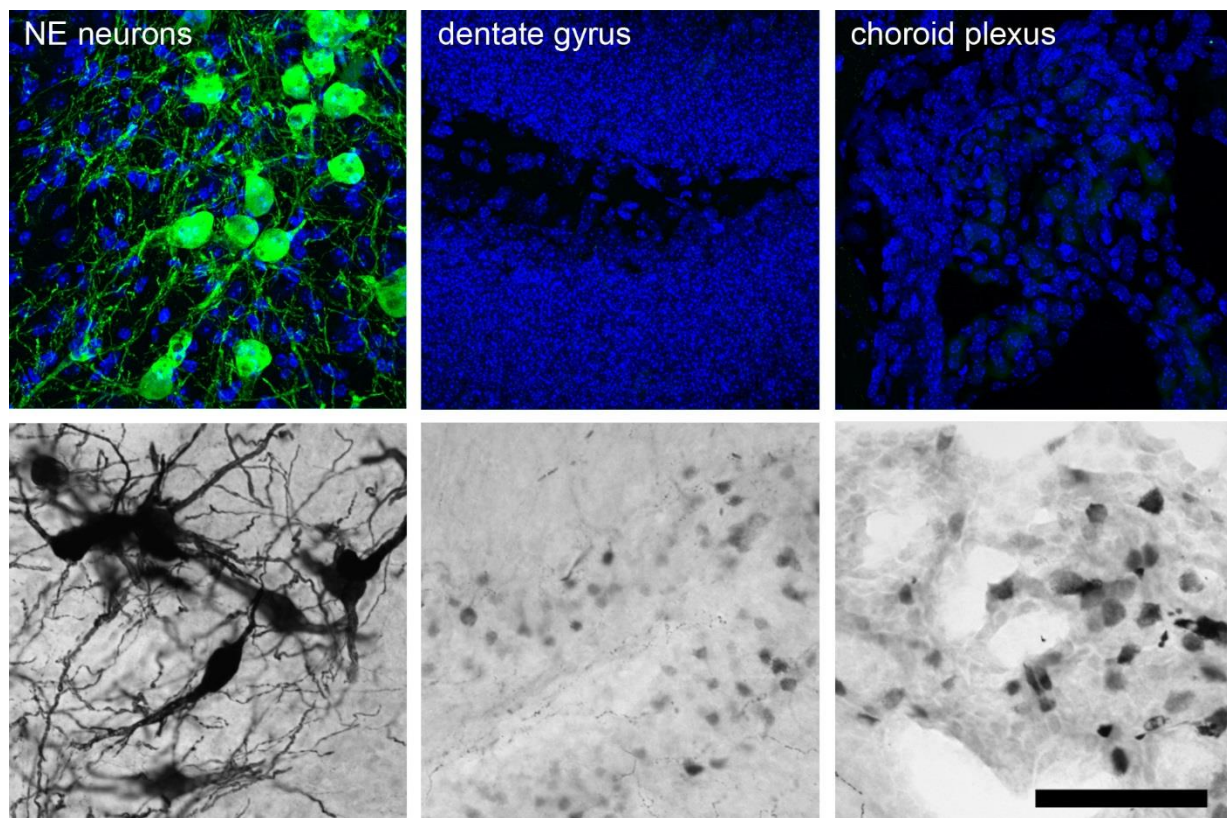
Fig. S2. eGFP expressed from *RC::RFLTG* after recombination is readily distinguished from very low level expression occurring in the absence of recombinases in choroid plexus and hippocampus.

eGFP expression in the brain of *En1^{Dre}; Dbh^{Flpo}; Gal-Cre; RC::RFLTG* mice was detected by immunohistochemistry using either a fluorescently labeled secondary antibody (top, n=10) or a horseradish peroxidase-coupled secondary antibody and fifteen minute incubation with the Vector SG chromogen for maximal staining (bottom, n=4). Noradrenergic (NE) neurons that have expressed all three recombinases are readily detected in the fluorescently labeled sample (top left), but eGFP is virtually undetectable in fluorescently labeled dentate gyrus (top center) and choroid plexus (top right) cells that have not expressed recombinases. Nuclear DAPI

fluorescence (blue) shows the presence of cells that are not otherwise labeled. Following the full fifteen minutes of chromogen precipitation, the staining is saturated in noradrenergic neurons (bottom left). Chromogen staining is much less dense in dentate gyrus (bottom center) and choroid plexus (bottom right) cells, allowing them to be readily distinguished from recombinase-expressing neurons (bottom left). Scale bar: 92 μm (top row) or 100 μm (bottom row).

Fig. S3: Immunostaining with anti-tryosine hydroxylase and anti-norepinephrine transporter antibodies confirms that intersectional crosses with *RC::FLTG* and *RC::RFLTG* efficiently label noradrenergic neurons.

Top row: In *En1^Cre^; Dbh^Flpo^; RC::FLTG* brain (n=4), noradrenergic neurons (locus coeruleus shown) with history of *En1* expression are labeled with eGFP, while those originating outside the *En1* expression domain are labeled with tdTomato. Co-labeling with an antibody against tyrosine hydroxylase (TH), an enzyme required for norepinephrine synthesis, confirms that recombination of *RC::FLTG* by these driver alleles efficiently labels the entire locus coeruleus. **Second row:** At projection target sites (hippocampus shown), co-labeling with an antibody against the norepinephrine transporter (NET) demonstrates that eGFP- and tdTomato-labeled axons originate from noradrenergic neurons. **Third row:** In *En1^Dre^; Dbh^Flpo^; Gal-Cre; RC::RFLTG* brain (n=4), only locus coeruleus neurons originating from the *En1* expression domain are labeled with eGFP (*Gal-Cre*-expressing) or tdTomato (*Gal-Cre*-negative). The very few locus coeruleus neurons originating outside the *En1* domain are labeled with anti-TH antibody, but neither eGFP nor tdTomato (blue neuron at left of asterisk). **Fourth Row:** At target sites of locus coeruleus projections (insular cortex shown), co-labeling with ant-NET demonstrates that eGFP- and tdTomato-labeled axons originate from noradrenergic neurons of the locus coeruleus complex. Images show immunofluorescence. Scale bar: 120 μm (locus coeruleus) or 20 μm (axons).
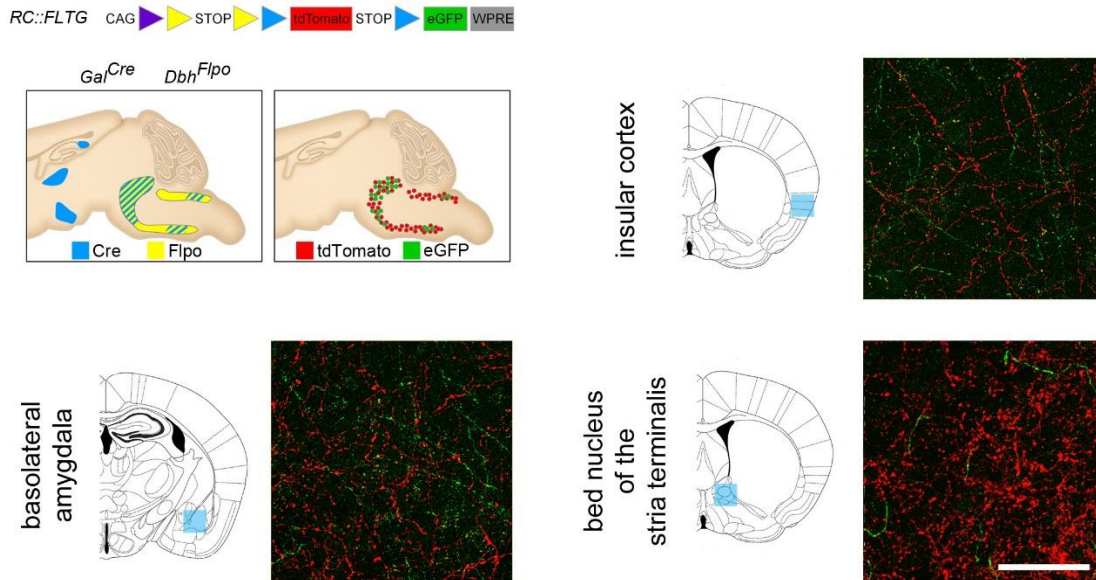
Fig. S4: Axons from all *Gal-Cre*-expressing and *Gal-Cre*-negative noradrenergic neurons can be labeled using a dual-recombinase responsive indicator allele.

In *Gal-Cre; Dbh^Flpo^; RC::FLTG* brain (n=4), *Gal-Cre*-expressing (eGFP-labeled) and *Gal-Cre*-negative (tdTomato-labeled) axons can be observed at target sites of noradrenergic projections. However, at sites which receive projections originating both within and outside the LC complex (e.g. insular cortex, amygdala, bed nucleus of the stria terminalis), *Gal-Cre*-expressing and *Gal-Cre*-negative axons from the LC complex cannot be distinguished from those originating in other noradrenergic subpopulations. Images show immunofluorescence. Scale bar: 50 μm
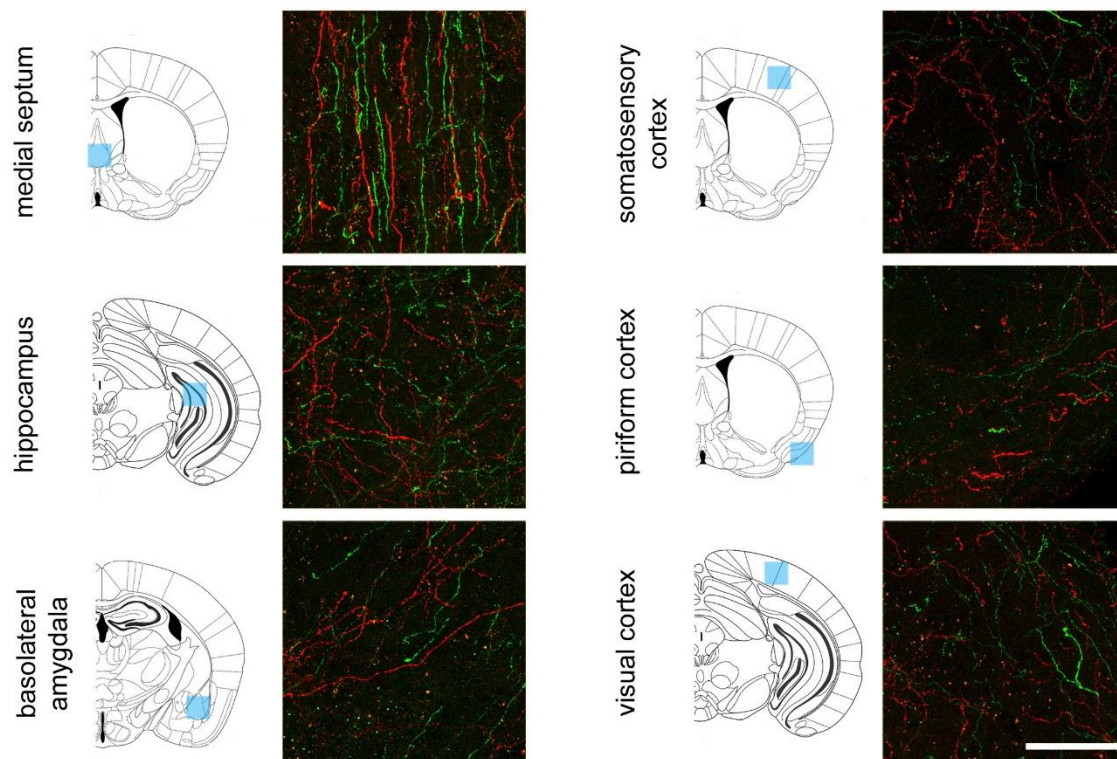
Fig. S5: Axons from *Gal-Cre*-expressing and *Gal-Cre*-negative neurons in the LC complex project to the same forebrain target regions.

In *En1^{Dre}; Dbh^{Flpo}; Gal-Cre; RC::RFLTG* quadruple heterozygous brain (n=10), eGFP-labeled (*Gal-Cre*-expressing) and tdTomato-labeled (*Gal-Cre*-negative) axons are observed intermingled at representative forebrain target sites. The blue boxes on the line diagrams show the approximate location of the imaged axons in coronal sections. Images show immunofluorescence. Scale bar: 50 μm
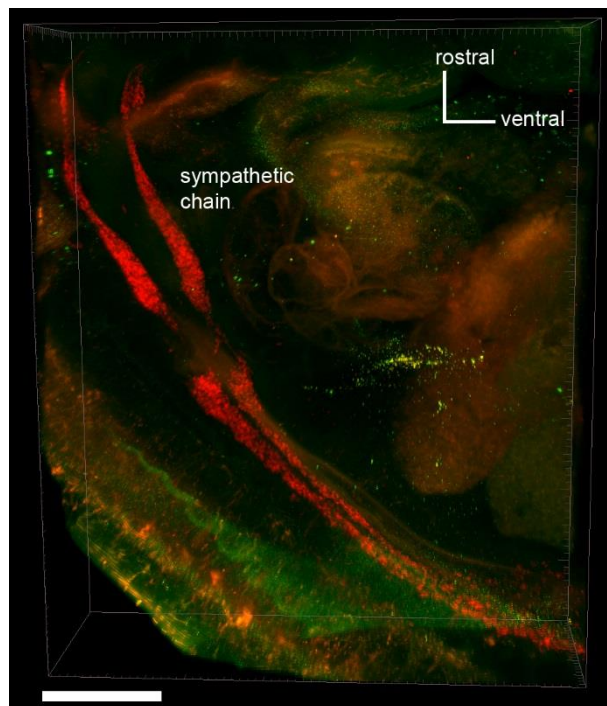
**Fig. S6. Labeled cells can be observed within intact embryos cleared by the passive clarity technique.**

tdTomato-labeled sympathetic ganglia are visible in the thoracic region of an E12.5 Dbh^{Flpo}; $RC::FLTG$ double heterozygous embryo (n=2) cleared with PACT. The intact shape and relative position of the bilaterally symmetric sympathetic chains can be clearly discerned. Image shows immunofluorescence. Scale bar: 600 µm.
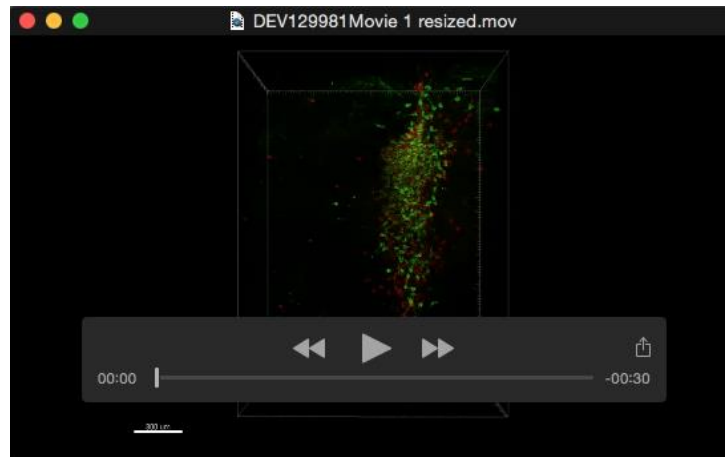
Movie 1. The intact structure of the locus coeruleus and dorsal subcoeruleus, and the spatial relationship of two subpopulations labeled with eGFP and tdTomato expressed from *RC::RFLTG*, are revealed in brain cleared by the passive clarity technique.

After PACT clearing and immunostaining of *En1^{Dre}*; *Dbh^{Flpo}*; *Gal-Cre*; *RC::RFLTG brain*, the morphology of the LC complex, divided into *Gal-Cre*-expressing (eGFP) and *Gal-Cre*-negative (tdTomato) subpopulations, can be observed. The neurons form a single, unbroken continuum extending from the densely packed locus coeruleus to the more loosely arranged subcoeruleus (see Fig. 5). *Gal-Cre*-expressing and *Gal-Cre*-negative noradrenergic neurons are intermingled throughout the structure, and a very few *Gal-Cre*-negative cells are widely displaced from the main body of neurons along the mediolateral axis. At the beginning of the movie, the rostral aspect of the population faces forward with the dorsal surface uppermost.

SUPPLEMENTARY MATERIALS AND METHODS

Generation of *RC::RFLTG* targeting vector

To facilitate insertion of three His3-SV40 transcriptional stop cassettes into the targeting vector, we first generated a version of pBS302 (Sauer, 1993) which lacks the *Mfe*I site in the SV40 poly(A) cassette. pBS302 was digested with *Mfe*I, the single strand overhang filled in, and the plasmid re-ligated. This modified pBS302 served as template for production of all three stop cassettes, as described below.

For the stop cassette following the tdTomato cDNA, the His3-Sv40 stop sequence was amplified with primers 5'-GACTAGTAGCTAGCAATTGTCGGGGACACCAAATATGGCGATC and 5'-GACTAGGAATTCTGATCATAGGTCCCTCGACCTGCAGCCCAAGC which contain *Eco*RI, *Mfe*I, and *Bcl*I sites. This PCR product was digested with *Eco*RI and *Mfe*I, and cloned into the *Eco*RI site of pRSET-tdTomato (Shaner et al., 2004). The tdTomato-stop was isolated by digestion with *Nhe*I and *Bcl*I and cloned into pL452 (Liu et al., 2003) digested with the same restriction enzymes. The resulting plasmid, ploxtdTomato, has loxP sites flanking tdTomato, His3-SV40 stop cassette, and bovine growth hormone (bGH) poly(A) cassette.

pCAG-GFP (Matsuda and Cepko, 2004), which has an enhanced green fluorescent protein gene controlled by CAG promoter (Niwa et al., 1991), was digested with *Not*I. The single-strand overhang was filled-in, and the plasmid was re-ligated to replace the *Not*I site with an *Fse*I site between the eGFP cDNA and β-globin polyadenylation cassette. ploxtdTomato was digested with *Spe*I and the single-strand overhang was filled in to generate a blunt end. The linearized plasmid was then digested with *Eco*RI, and the loxP-flanked tdTomato-His3-SV40 stop-bGH poly(A) was cloned between the *Sma*I and *Eco*RI sites of the modified pCAG-GFP to generate pCAG-loxTloxG.

The FRT-flanked His3-SV40 stop cassette was amplified from the modified pBS302 using primers 5'- GACTAGGAATTC<u>GAAGTTCCTATTCTCTAGAAAGTATAGGAACTTC</u>TCGG GGACACCAAATATGGCGATC and 5'- GACTAGTAGCTAGCAATTGATGCAT<u>GAAGTTCC TATACTTTCTAGAGAATAGGAACTTC</u>TAGGTCCCTCGACCTGCAGCCCAAGC. The primers contain FRT sites (underlined) and *Eco*RI, *Mfe*I and *Nsi*I sites for subsequent cloning. The rox-flanked stop cassette was amplified with primers 5'-GACTGAATTC<u>TAACTTTAAATAATGCCAAT TATTTAAAGTTA</u>TCGGGGACACCAAATATGGCGATC and 5'-GACTGACTCAATTG<u>TAACTTTA AATAATTGGCATTATTTAAAGTTA</u>TAGGTCCCTCGACCTGCAGCCCAAGC. The primers contain rox sites (underlined) and *Eco*RI and *Mfe*I sites for cloning. The FRT-flanked and rox-flanked cassettes were digested with *Eco*RI and *Mfe*I and cloned sequentially into the *Eco*RI site of the pCAG-loxTloxG to generate pCAG-RFLTG.

A *Spe*I-*Pac*I-*Avr*II linker was generated by annealing oligonucleotides with the sequence 5'-CTAGTTTAATTAAC and 5'-CTAGGTTAATTAAA and cloned into the *Spe*I site upstream of the CAG promoter. An *Eco*RI-*Mlu*I-*Mfe*I linker was generated by annealing 5'-AATTCACGCGTC and 5'- AATTGACGCGTG and cloned into the *Eco*RI site downstream of the CAG promoter. Finally, the CAG promoter, STOP cassettes, and fluorophore cDNAs were all isolated in a single fragment by digestion with *Pac*I and *Fse*I and cloned into pAi9 (Madisen et al., 2010) digested with the same two enzymes to generate the *Gt(ROSA)26Sor* targeting vector, pRC-RFLTG (p**R**osa-**C**AG-**r**ox-**F**RT-**l**oxP-td**T**omato-e**G**FP). The digested fragment of pAi9 provided the woodchuck hepatitis virus posttranscriptional regulatory element (WPRE) (Zufferey at al., 1999) and bGH poly(A) cassette that follow the eGFP cDNA, the 5' and 3' homology to the *Gt(ROSA)26Sor* locus (Friedrich and Soriano, 1991), attB/attP-flanked Neo cassette, and diphtheria toxin (DTA) cassette for negative selection in embryonic stem cells. The WPRE is not expected to have any effect on expression of tdTomato, because a stop cassette is

located between the tdTomato and eGFP cDNAs. pRC-RFLTG has unique *Kpn*I, *Pac*I, *Mlu*I, *Fse*I, and *Asc*I sites to facilitate additional modification. For transformation of ES cells, the vector was linearized with *Kpn*I.

PACT tissue clearing and immunofluorescence

For the passive clarity technique, we followed the previously published protocol (Yang et al., 2014). Mice were perfused and brains post-fixed overnight in 4% PFA as described above. After rinsing in PBS, brains were cut into four 3 mm-thick coronal slices using a brain matrix. The slices were embedded in 4% polyacrylamide gel (A4P0) and lipids were extracted by incubation in 8% SDS at 37 °C for four days. Cleared brain slices were washed five times in PBS for 1 hour each rinse at room temperature and then washed overnight in PBS with 0.01% sodium azide. Prior to addition of antibodies, slices were incubated in PBS with 0.1% Triton X-100 (PBST), 5% donkey serum and 0.01% sodium azide for 24 hours at room temperature. The slices were then incubated in PBST with primary antibodies, 2% donkey serum, and 0.01% sodium azide on an orbital shaker at room temperature. The rabbit anti-dsRed antibody was used at 1:500 dilution and the chicken anti-GFP at 1:1000. The buffer and antibodies were replaced with fresh solution after three days, and after a total of five days incubation, the slices were rinsed in PBST and washed overnight in PBST with 0.1% sodium azide. The following day, the slices were washed 5 more times in PBST for one hour each wash and then incubated at room temperature in PBST with Alexa Fluor 568 donkey anti-rabbit F(ab')2 fragments (1:500), Alexa Fluor 488 donkey anti-chicken F(ab')2 fragments (1:500), 2% donkey serum, and 0.01% sodium azide. Buffer and antibodies were replaced with fresh solution after three days and the incubation continued for two more days. The slices were washed five times in PBST for one hour each and

then washed overnight in PBS at 4 °C. The following day, the slices were transferred to RIMS (Yang et al., 2014). After overnight incubation at 4 °C, the slices were mounted in fresh RIMS between two coverslips separated by a 3 mm iSpacer (SunJin Lab Company, Hsinchu City, Taiwan) and imaged. E12.5 embryos were fixed by immersion overnight in 4% PFA in PBS, embedded in A4P0, and cleared in 8% SDS for 14 hours at room temperature. After the embryos were rinsed in PBS, immunofluorescent labeling and mounting in RIMS was performed as described for brain slices.

SUPPLEMENTARY REFERENCES

Friedrich, G., and Soriano, P. (1991). Promoter traps in embryonic stem cells: a genetic screen to identify and mutate developmental genes in mice. *Genes Dev.* **5**, 1513-1523.

Liu, P., Jenkins, N. A., and Copeland, N. G. (2003). A highly efficient recombineering-based method for generating conditional knockout mutations. *Genome Res.* **13**, 476-484.

Madisen, L., Zwingman, T. A., Sunkin, S. M., Oh, S. W., Zariwala, H. A., Gu, H., Ng, L. L., Palmiter, R. D., Hawrylycz, M. J., Jones, A. R., Lein, E. S., and Zeng, H. (2010). A robust and high-throughput Cre reporting and characterization system for the whole mouse brain. *Nat. Neurosci.* **13**, 133-140.

Matsuda, T., and Cepko, C. L. (2004). Electroporation and RNA interference in the rodent retina in vivo and in vitro. *Proc. Natl. Acad. Sci. USA* **101**, 16-22.

Niwa, H., Yamamura, K., and Miyazaki, J. (1991). Efficient selection for high-expression transfectants with a novel eukaryotic vector. *Gene* **108**, 193-199.

Sauer, B. (1993). Manipulation of transgenes by site-specific recombination: use of Cre recombinase. *Methods Enzymol.* **225**, 890-900.

Shaner, N. C., Campbell, R. E., Steinbach, P. A., Giepmans, B. N., Palmer, A. E., and Tsien, R. Y. (2004). Improved monomeric red, orange and yellow fluorescent proteins derived from Discosoma sp. red fluorescent protein. *Nature Biotechnol.* **22**, 1567-1572.

Yang, B., Treweek, J. B., Kulkarni, R. P., Deverman, B. E., Chen, C. K., Lubeck, E., Shah, S., Cai, L., and Gradinaru, V. (2014). Single-cell phenotyping within transparent intact tissue through whole-body clearing. *Cell* **158**, 945-958.

Zufferey, R., Donello, J. E., Trono, T. J., and Hope, T. J. (1999). Woodchuck hepatitis virus posttranscriptional regulatory element enhances expression of transgenes delivered by retroviral vectors. *J. Virol.* **73**, 2886-2892.